

45. *Behavior of Solid Friction in a Seismic System with  
One Degree of Freedom under Harmonic  
External Force.*

By Genrokuro NISHIMURA,  
Earthquake Research Institute  
and  
Tomio KOTAKI,  
Chuo University.

(Read March 24, 1964.—Received Aug. 20, 1965.)

Introduction

Concerning the stationary motion of a seismic system with one degree of freedom subjected to both solid and fluid frictions and a harmonic external force, the existence of the following three phases of vibrations has already been announced by J. P. Den Hartog<sup>1)</sup>, T. Hagiwara<sup>2)</sup> and Thomas A. Parls and Emile S. Herrard<sup>3)</sup>: (1) The motion is a continuous vibration with instantaneous stop when the amplitude of the external force is very large in comparison with the solid friction. (2) When the force amplitude is not so large, however, a temporary stop with finite time interval may arise in the vibration during its half period. (3) In the case when the force amplitude becomes very small as compared with the frictional force, the system is always at rest.

Now, the equation of motion of the system can be expressed as

$$m \frac{d^2x}{dt^2} + 2b \frac{dx}{dt} + kx = r + f \cdot \cos(pt + \alpha), \quad (1)$$

where  $x$  is the displacement of the concerned system,  $t$  the time,  $m$  and  $k$  the mass and the spring constant of the system,  $b$  the coefficient of fluid friction,  $f$ ,  $p$  and  $\alpha$  the amplitude, the circular frequency and the phase angle of the external force respectively. Symbol  $r$  represents the solid frictional force, and particularly in the state of motion, we can assume it as under:

$$r = -r_0 S \left[ \frac{dx}{dt} \right]. \quad (2)$$

1) J. P. Den HARTOG, *Phil. Mag.*, **9** (1930), 801.

2) T. HAGIWARA, *Bull. Earthq. Res. Inst.*, **11** (1933), 14.

3) THOMAS A. PARLS and Emile S. HERRARD, *Jour. Res. of N. B. S. in U. S. A.* **57** (1956), 2693.

Here,  $r_0$  is the absolute value of the solid friction in the state of motion and  $S$  is a symbolical function, taking the value of  $+1$  or  $-1$  when the value in parenthesis [ ] becomes positive or negative respectively. Thus, we can write as follows :

$$\left. \begin{array}{l} \text{When } (dx/dt) > 0, \quad S = +1, \\ \text{and when } (dx/dt) < 0, \quad S = -1. \end{array} \right\} \quad (3)$$

When the system comes to a standstill, the value of the solid friction has to be determined by balancing the condition of forces. Using Eq. (1), we can obtain the value of  $r$  at rest as follows :

$$\text{When } (dx/dt) = 0, \quad r = kx_0 - f \cdot \cos(pt + \alpha), \quad (4)$$

where  $x_0$  is the displacement during a rest.

The method taken by J. P. Den Hartog<sup>4)</sup> is to confine the problem only in a zone of  $S$  having the same sign for deriving general solution, and to obtain the solution by determining two integral constants corresponding to the condition for the steady motion. The method of T. Hagiwara<sup>5)</sup> is, availing of the fact that the velocity changes its sign before and after a point of time where an expected solution for steady motion becomes maximum, to convert the solid friction  $r$  represented in Eq. (1) to a continuous function of time by using Fourier Series, which becomes a single differential equation, thus enabling a solution. The above two authors, however, did not taken up the condition of solid friction expressed by (4), and obtained only the solution for continuous vibration. Thomas A. Parls and Emile S. Herrard<sup>6)</sup>, considering the condition (4), have traced the solution of the equation of motion by using an analog computer, and thereby obtained the stationary solution with temporary stop when the force amplitude is not so large.

Now, the method developed in Part I of this paper is, starting from an arbitrary initial condition, to follow the successive calculation to arrive finally at the desired solution for steady motion. As actual calculation is too complex, however, an attempt is made to solve the problem by a graphical method introducing the concept of topological space. In Part II, an analytical method is applied to solve the problem, starting from the solution directly derived from the equation of motion. The other analytical method is developed in Part III by means of Fourier series

4) *loc. cit.*, 1).

5) *loc. cit.*, 2).

6) *loc. cit.*, 3).

to solve the same problem. In Parts II and III, a finite time interval of stop is assumed during a period of vibration where the force amplitude is not so large.

Part I. Theory of Graphical Approach

CHAPTER I. THEORY OF GRAPHICAL METHOD

1.1. Solution of Equation

For non-dimensional expression, let us rewrite Eq. (1) as

$$\ddot{y} + 2h\dot{y} + y = R + g \cdot \cos(\gamma\tau + \alpha), \tag{5}$$

where  $\tau = nt, \quad n = \sqrt{\frac{k}{m}}, \quad y = \frac{kx}{r_0}, \quad R = \frac{r}{r_0}, \quad g = \frac{f}{r_0}, \quad \gamma = \frac{p}{n}, \tag{6}$

and dot means differentiation with regard to  $\tau$ . By using these notations, the expressions for solid friction (2) and (4) become as follows: When it is in motion,

$$R = -S[\dot{y}], \tag{7}$$

and when it is at rest,

$$R = y_0 - g \cos(\gamma\tau + \alpha). \tag{8}$$

Solution of Eq. (5) can be expressed in the following form:

$$y = A \exp(-h\tau) \cos(\nu\tau + \epsilon) - S[\dot{y}] + \frac{G}{\gamma} \cos(\gamma\tau + \alpha + \beta), \tag{9}$$

where  $\nu = \sqrt{1 - h^2}, \tag{10}$

$$\sin \beta = -2h\gamma e \quad \cos \beta = (1 - \gamma^2)e, \tag{11}$$

$$e = \frac{1}{\sqrt{(1 - \gamma^2) + (2h\gamma)^2}}, \tag{12}$$

$$G = \gamma g e, \tag{13}$$

and  $A$  and  $\epsilon$  are constants to be determined by the initial conditions.

Let us differentiate Exp. (9). Then, we have

$$\dot{y} = A \exp(-h\tau) \cos(\nu\tau + \epsilon + \sigma) - G \sin(\gamma\tau + \alpha + \beta). \tag{14}$$

Now, rewrite Exps. (9) and (14) as

$$y = u + \frac{v}{\gamma}, \quad (15)$$

$$\dot{y} = \dot{u} + \frac{\dot{v}}{\gamma}, \quad (16)$$

where

$$u = A \exp(-\nu\tau) \cos(\nu\tau + \varepsilon) - S[\dot{y}], \quad (17)$$

$$\dot{u} = A \exp(-h\tau) \cos(\nu\tau + \varepsilon + \sigma), \quad (18)$$

$$v = G \cos(\nu\tau + \alpha + \beta), \quad (19)$$

$$\dot{v} = -\gamma G \varepsilon \sin(\nu\tau + \alpha + \beta), \quad (20)$$

in which

$$\cos \sigma = -h, \quad \sin \sigma = \nu. \quad (21)$$

### 1.2. Topological Plane ( $u-\dot{u}$ )

As shown in Fig. 1, an axis  $\dot{u}$  is taken as abscissa and  $u$ -axis is taken in the direction which makes angle  $\sigma$  with  $\dot{u}$ -axis. Then let us consider a plane of oblique co-ordinate  $(u, \dot{u})$  and plot on the plane a point represented by Exps. (7) and (18) with  $\tau$  as a parameter. Then, we have as its locus two logarithmic spirals having their centers at  $u = +1$  and  $u = -1$  according to the sign of  $S$  in Exp. (17), which can be indicated by the following expression in which  $\rho$  is a radius and  $\theta$  is an angle measured in an anti-clockwise direction:

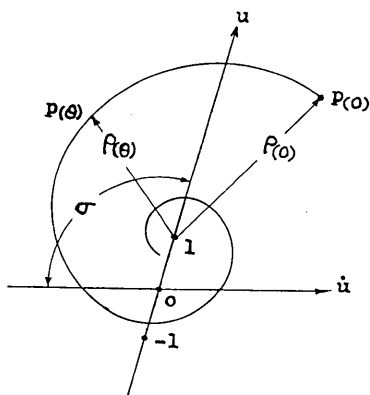


Fig. 1.

$$\rho_{(\theta)} = A\nu \exp\left(\frac{-h\theta}{\nu}\right). \quad (22)$$

The variable angle  $\theta$  in this expression can be connected with  $\tau$  as

$$\theta = \nu\tau \quad (23)$$

What is concerned in the current discussion is the value of  $y$ , that is, the motion of the mass, and it can be determined by the values of  $u$  and  $v$ . In this regard,  $v$ -axis is taken normal to  $u-\dot{u}$  plane, in which  $v$  is a function of  $\tau$  as indicated by Exp. (19), thereby, a point having co-ordinates  $u, \dot{u}$  and  $v$  traces a space curve in the topological space  $u-\dot{u}-v$  thus established and the vibration of the mass under consideration

7) The mathematical proof in this regard can be obtained by referring to; FLÜGGE-Lortz, I, "Discontinuous Automatic Control", Princeton Univ. Press, 1953.

can be completely represented by the displacement of the point on the space curve. Logarithmic spiral on  $u-\dot{u}$  plane is the projection of this space curve on the plane.

1.3. Topological Plane ( $\dot{u}-v$ )

As already discussed, the center of the logarithmic spiral projected on  $u-\dot{u}$  plane changes to the location  $u=-S[\dot{y}]$  according to the sign of  $\dot{y}$ ; simultaneously, it may be possible that the topological curve in the space would also change its location. In order to clarify this question, convert the form of  $\dot{v}$  in Exp. (20) to

$$\dot{v} = \gamma \sqrt{G^2 - v^2} S[\dot{v}]. \tag{24}$$

Since the value of root form in Exp. (24) cannot be made greater than that of  $G$ , we see that

$$\left. \begin{array}{l} \text{when } \dot{u} > G, \quad \dot{y} > 0, \\ \text{and when } \dot{u} < -G, \quad \dot{y} < 0. \end{array} \right\} \tag{25}$$

Now, let us obtain the boundary at which  $\dot{y}$  changes its sign. This changing will be called "switching". The condition of switching is

$$\dot{y} = 0, \tag{26}$$

thus, using Exps. (16) and (24), we have

$$\dot{u} + \sqrt{G^2 - v^2} S[\dot{v}] = 0. \tag{27}$$

This equation represents two semi-circles of radius  $G$  with their centers at the origin, and one locates on the right-zone and the other the left-zone of  $v$ -axis as a boundary line. As can be seen from the inequalities shown by (25), with these semi-circles as a boundary,  $\dot{y}$  becomes negative

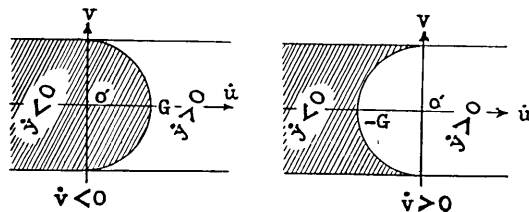


Fig. 2.

where  $\dot{u}$  is in the region of smaller value and becomes positive where  $\dot{u}$  is in the region of greater value, Fig. 2 illustrating these relationships.

The topological curve  $\dot{u}-v$  obtained by projection of the space curve on

the plane can be expressed as follows with  $\theta$  as parameter:

$$\dot{u} = A \exp\left(-\frac{h\theta}{\nu}\right) \cos(\theta + \varepsilon + \sigma), \tag{28}$$

$$v = G \cos(\mu\theta + \alpha + \beta), \tag{29}$$

where 
$$\mu = \frac{\gamma}{\nu}. \tag{30}$$

This curve can be traced by the graphical method, which will be fully discussed afterwards. Anyway, the switching should occur at the very moment when the topological curve on the concerned plane intersects with the semi-circles.

1.4. Method of tracing Topological Curve

As a preparation, draw two planes  $u-\dot{u}$  and  $\dot{u}-v$  as indicated in Fig. 3. Radius  $G$  of switching circle and oblique angle  $\sigma$  are obtainable from the constants of the concerned system and the form of spiral curve is determined by using these constants. Now, let us start from initial values of  $u_0$ ,  $\dot{u}_0$  and  $v_0$ , provided that the absolute value of  $v_0$  should be made smaller than  $G$ . With these initial values, a point  $p_0$  can be determined on  $u-\dot{u}$  plane and corresponding point  $p'_0$  on  $\dot{u}-v$  plane.

Exp. (29) indicates that the vibration of  $v$  is a cosine function with amplitude  $G$  and variable angle  $\mu\theta$ . Thence, let us consider an imaginary circle of radius  $G$  with its center at the point  $o'$  and let a point  $q$  be rotating about the circumference with angular displacement  $\mu\theta$  from a point  $q_0$  as the starting point. Then, the projection of point  $q$  on  $v$ -axis is the value of

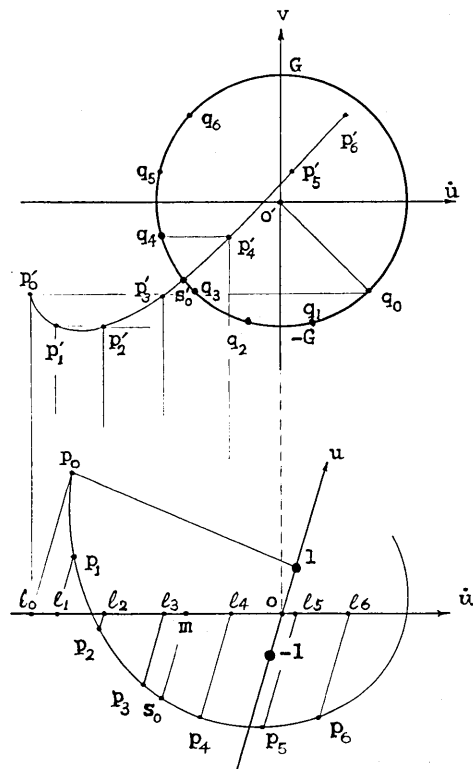


Fig. 3.

$v$ , as seen from Exp. (29). With such a consideration that the variation of  $v$  is produced by that of  $q$ , the curve tracing may become easier. In this case, rotational direction of  $q$  should be made clockwise, and this reason will be explained afterwards. As  $\dot{u}$  and  $\dot{v}$  are both negative in the current case,  $\dot{y}$  also becomes negative by Exp. (16) and the spiral center falls in  $u=+1$ . We can thus draw a spiral curve having its center at  $u=+1$  and passing through  $p_0$ . Drawing a line connecting two points  $p_0$  and  $u=+1$  as a basic starting line, divide the curve at a constant angular interval  $\Delta\theta$  (say  $20^\circ$ ) as shown by points  $p_1, p_2, \dots$ . Through these points, draw each parallel line to  $u$ -axis and let  $l_1, l_2, l_3, \dots$  be the intersecting points of  $\dot{u}$ -axis with these lines. On the other hand, make a similar circular division at a constant angular interval  $\Delta\mu\theta$  (say  $30^\circ$ ) on the circle of radius  $G$  in a clockwise direction starting from a line  $o'q_0$  as a basis as shown by points  $q_1, q_2, \dots$ . And through these points, draw each parallel line to  $\dot{u}$ -axis and let these lines be intersected with those drawn normal to  $\dot{u}$ -axis through points  $l_1, l_2, l_3, \dots$ . A point  $p'_1$  is an intersecting point of two lines, one from  $q_1$  and the other from  $l_1$  thus drawn as above,  $p'_2$  corresponds to an intersecting point of lines through  $q_2$  and  $l_2$ , in the same way, the following intersecting points  $p'_3, p'_4, \dots$  are thus graphically obtained. Now, connecting each point  $p'_0, p'_1, p'_2, \dots$  by using a curve ruler, we can obtain topological curve with regard to  $\dot{u}$ - $v$  plane.

It is of note, however, that if the topological curve intersects with the circumference, the semi-circle in which the switching should occur becomes different according to what sign  $\dot{v}$  should have at the point of such intersection. Under the current status,  $\dot{v}$  is positive when switching takes place, thus the concerned semi-circle is that located in the left-zone and the intersecting point  $s'_0$  with this semi-circle is the switching point of the  $\dot{u}$ - $v$  plane. Denote  $m$  an intersecting point of  $\dot{u}$ -axis with a parallel line to  $v$ -axis through  $s'_0$ , and  $s_0$  an intersecting point of spiral curve with a line parallel to  $u$ -axis through  $m$ , then a point  $s_0$  becomes the switching point with regard to  $u$ - $\dot{u}$  plane as shown in Fig. 3.

Thus far we have discussed the procedure of tracing a topological curve to obtain the switching point, and now we are in a position to go into the method of tracing the topological curve after a switching and this will be fully treated in the following chapter.

## CHAPTER II. TOPOLOGICAL CURVE AFTER SWITCHING

## 2.1. Motion after Switching

In preceding Chapter I, the method of obtaining the switching point was fully discussed. To locate such a point means to determine the time at which switching occurs. When it takes place, the velocity of the system becomes zero. In order to study the nature of motion that would occur after switching, it is required to take into account an effect of solid friction when the system is at rest.

A solid body would start its motion when it is subjected to an external force of a magnitude greater than that of  $r$  defined in the preceding section of this paper. Now, the force under consideration is expressed in the term of

$$f \cos (pt + \alpha) - kx .$$

Let us denote the switching time as  $t_0$  and add symbol "o" to all notations relating to the time. Then the condition of starting motion can be mathematically presented by

$$|f \cos (pt_0 + \alpha) - kx_0| > r_0 , \quad (31)$$

and its corresponding acceleration is given by

$$\left( m \frac{d^2x}{dt^2} \right)_0 = f \cos (pt_0 + \alpha) - kx_0 - r_0 S[f \cos (pt_0 + \alpha) - kx_0] . \quad (32)$$

When this acceleration has a positive sign, the corresponding velocity thereafter also becomes positive and *vice-versa*. Thus the sign of velocity after switching is determined by that of the right-hand side of Exp. (32), that is,

$$S \left[ \frac{dx}{dt} \right]_{t > t_0} = S[f \cos (pt_0 + \alpha) - kx_0 - r_0 S[f \cos (pt_0 + \alpha) - kx_0]] ,$$

and also the following equation is justified in consideration of relationship (31):

$$S \left[ \frac{dx}{dt} \right]_{t > t_0} = S[f \cos (pt_0 + \alpha) - kx_0] . \quad (33)$$

Fig. 4 (a) illustrates the case of the condition (31), and Fig. 4 (b) indicates the case of

$$|f \cos (pt_0 + \alpha) - kx_0| < r_0 . \quad (34)$$

In the case of the above condition, a body would continue to be at rest,



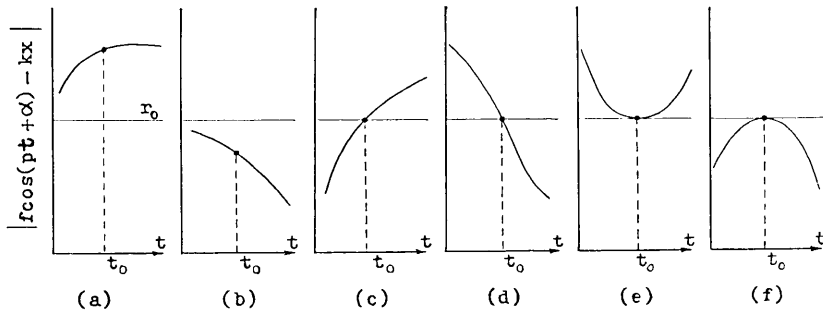


Fig. 4.

even though it is acted upon by an external force, of which magnitude is smaller than that of  $r_0$ . The motion, however, will be resumed when the condition satisfied by (31) comes into existence in the course of time.

When the following condition is satisfied:

$$|f \cos (pt_0 + \alpha) - kx_0| = r_0, \tag{35}$$

four cases are to be considered as indicated by Fig. 4 (c), (d), (e) and (f). For the case (c),

$$\left\{ \frac{d}{dt} |f \cos (pt + \alpha) - kx_0| \right\}_{t_0} > 0 .$$

This means

$$\{f \cos (pt_0 + \alpha) - kx_0\} \sin (pt_0 + \alpha) < 0 , \tag{36}$$

and the acceleration and the velocity develops immediately after switching, the motion then continuing. The sign of the velocity at the concerned stage can be expressed in the same form as (33).

For the case (d),

$$\left\{ \frac{d}{dt} |f \cos (pt + \alpha) - kx_0| \right\}_{t_0} < 0 ,$$

and this means

$$\{f \cos (pt_0 + \alpha) - kx_0\} \sin (pt_0 + \alpha) > 0 , \tag{37}$$

the motion being brought to a stop after switching as Fig. 4 (d) shows.

For cases (e) and (f),

$$\left\{ \frac{d}{dt} |f \cos (pt + \alpha) - kx_0| \right\}_{t_0} = 0 ,$$

and then, we have

$$\sin (pt_0 + \alpha) = 0. \quad (38)$$

For case (e), however, the following relationship must be satisfied in addition to (35) and (38):

$$\left\{ \frac{d^2x}{dt^2} |f \cos (pt + \alpha) - kx_0| \right\}_{t_0} > 0,$$

from which we have

$$\{f \cos (pt_0 + \alpha) - kx_0\} \cos (pt_0 + \alpha) < 0. \quad (39)$$

The motion under this condition continues, and its sign of velocity can also be determined from (33). For the case (f), in the same way, an additional condition required besides (35) and (38) is

$$\{f \cos (pt_0 + \alpha) - kx_0\} \cos (pt_0 + \alpha) > 0. \quad (40)$$

The motion corresponding to the cases indicated by Figs. 4 (d) and (f) may stop after switching in the same manner as in the case of (b), the system remaining at rest unless the condition (31) makes its appearance.

Table 1.

Condition		Motion after switching	
$ w_0  \neq 1$	$ w_0  > 1$	start	
	$ w_0  < 1$	stop	
$ w_0  = 1$	$\sin (\mu\theta_0 + \alpha) \neq 0$	$w_0 \sin (\mu\theta_0 + \alpha) < 0$	start
		$w_0 \sin (\mu\theta_0 + \alpha) > 0$	stop
	$\sin (\mu\theta_0 + \alpha) = 0$	$w_0 \cos (\mu\theta_0 + \alpha) < 0$	start
		$w_0 \cos (\mu\theta_0 + \alpha) > 0$	stop

All expressions of conditions developed thus far can be rewritten by those notations introduced in the preceding chapter. The results of comparison made on each other after re-arrangement are shown in Table 1, in which  $w_0$  means that

$$w_0 = \eta_0 - \gamma_0, \quad (41)$$

where  $\eta_0 = g \cos (\mu\theta_0 + \alpha), \quad (42)$

and  $\gamma_0 = u_0 - \frac{v_0}{\gamma}. \quad (43)$

The value of  $u_0$ ,  $v_0$  and  $\mu\theta_0 + \alpha$  in above expressions can be obtained from the position of switching points  $s_0$  and  $s'_0$ .

Should the motion continue after switching, the sign of the velocity is totally determined by the following equation rewritten from (33):

$$S[y_{\theta > \theta_0}] = S[w_0]. \tag{44}$$

2.2. Graphical Method of Discriminating Conditions

Various relationships to discriminate how the motion continues after switching and also what sign its corresponding velocity would take, were derived in the preceding paragraph. Now, the method of graphical discrimination will be developed.

Let us consider a rectangular co-ordinate parallel to  $u$ - and  $v$ -axis and rotate it by angle  $\beta$  in a clockwise direction. Then, we can establish a new system of co-ordinates  $\xi$ ,  $\eta$  as shown in Fig. 5 with positive

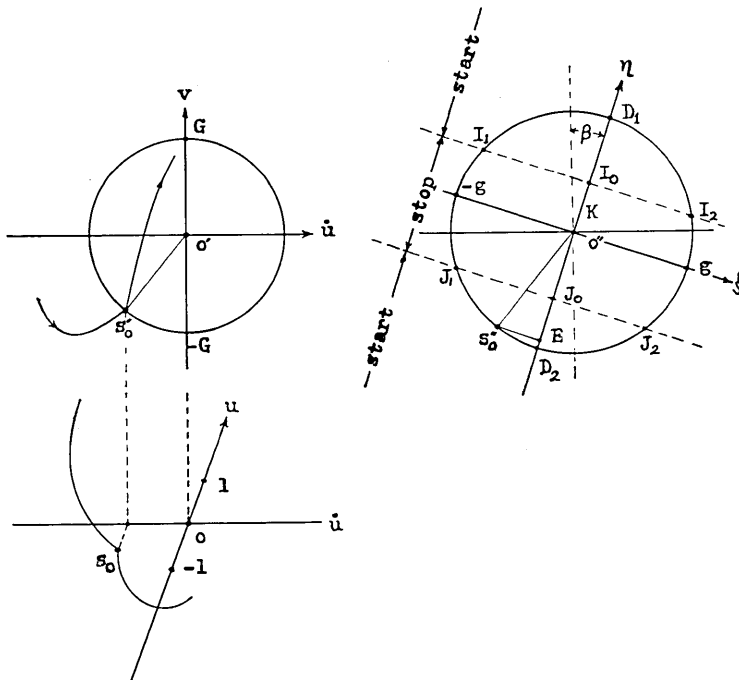


Fig. 5.

direction as the arrow indicates. With  $o''$  as the origin, draw a circle of radius  $g$  and let  $D_1$  and  $D_2$  be intersecting points of this circle with

$\eta$ -axis. A point  $s_0''$  is an intersection of the circle with a line parallel to  $o's_0'$  through  $o''$ . Then,

$$\angle D_1 o'' s_0'' = \mu\theta_0 + \alpha.$$

Denoting the projecting point of  $s_0''$  on  $\eta$ -axis as  $E_0$ , we have

$$o''E_0 = g \cos(\mu\theta_0 + \alpha) = \gamma_0. \quad (45)$$

Next, from two intersecting points  $s_0$  and  $s_0'$ , we can obtain the value of  $y_0$  through Exp. (43). By using this value, three points  $I_0$ ,  $J_0$  and  $K_0$  can be located on  $\eta$ -axis through following calculation:

$$\left. \begin{aligned} o''I_0 &= y_0 + 1, \\ o''J_0 &= y_0 - 1, \\ o''K_0 &= \gamma_0 - y_0 = w_0. \end{aligned} \right\} \quad (46)$$

Moreover, the condition  $|w_0| > 1$  in Table 1 is rewritten into

$$y_0 - 1 > \gamma_0, \quad \text{or} \quad y_0 + 1 < \gamma_0,$$

and the condition  $|w_0| < 1$  becomes

$$y_0 - 1 < \gamma_0 < y_0 + 1.$$

These satisfy the condition that the motion stops if  $E_0$  locates between  $I_0$  and  $J_0$ , and it starts if  $E_0$  exists in the exterior zone of  $I_0$  and  $J_0$ .

When the point  $E_0$  coincides either with  $I_0$  and  $J_0$ , what does it come out as thereafter? If  $E_0$  coincides with  $I_0$ , then,

$$\left. \begin{aligned} \gamma_0 - y_0 = w_0 = 1. \\ \text{If } E_0 \text{ coincides with } J_0, \text{ then,} \\ \gamma_0 - y_0 = w_0 = -1. \end{aligned} \right\} \quad (47)$$

For either case, it becomes  $|w_0| = 1$ . Assuming that both points  $I_0$  and  $J_0$  are included in the circle, let  $I_1$ ,  $I_2$  and  $J_1$ ,  $J_2$  be such points of intersection of the circle with a normal line drawn to  $\eta$ -axis through  $I_0$  and  $J_0$  as shown in Fig. 5. In the case that  $I_0$  or  $J_0$  comes out of the circle, however,  $I_1$  and  $I_2$  or  $J_1$  and  $J_2$  do not exist. When  $s_0''$  coincides with,

$$\left. \begin{aligned} \text{either } I_1 \text{ or } J_1, \text{ then, } \sin(\mu\theta_0 + \alpha) < 0, \\ \text{and either } I_2 \text{ or } J_2, \text{ then, } \sin(\mu\theta_0 + \alpha) > 0. \end{aligned} \right\} \quad (48)$$

The combination of two relationships (47) and (48) all together leads to that, when  $s_0''$  coincides either with  $I_1$  or  $J_2$ , the motion starts, since

$$w_0 \sin (\mu\theta_0 + \alpha) < 0,$$

when it coincides either with  $I_2$  or  $J_1$ , the motion stops, since

$$w_0 \sin (\mu\theta_0 + \alpha) > 0.$$

When  $I_0$  or  $J_0$  coincides with  $D_1$  or  $D_2$ , and also with  $s_0''$ , it means that  $\sin (\mu\theta_0 + \alpha) = 0$ , from which it can be deduced that

$$\left. \begin{array}{l} \text{at point } D_1, \quad \cos (\mu\theta_0 + \alpha) = 1, \\ \text{and at point } D_2, \quad \cos (\mu\theta_0 + \alpha) = -1. \end{array} \right\} \quad (49)$$

Again, combining the two relationships (47) and (49), the results are such that, when  $s_0''$ ,  $D_1$ ,  $J_0$  or  $s_0''$ ,  $D_2$ ,  $I_0$  become coincident with one another, the motion starts since  $w_0 \cos (\mu\theta_0 + \alpha) < 0$ , and when  $s_0''$ ,  $D_1$ ,  $I_0$  or  $s_0''$ ,  $D_2$ ,  $J_0$  do, it stops since  $w_0 \cos (\mu\theta_0 + \alpha) > 0$ .

In order to summarize all that has been discussed thus far, let  $\xi$ - $\eta$  plane be provided with certain characteristics. As we considered the point  $q$  in  $u$ - $v$  plane, that is, rotating on the circle at angular displacement  $(\mu\theta + \alpha + \beta)$ , in the same way we consider the equivalent point  $e$  in  $\xi$ - $\eta$  plane, that is, rotating on the circle with radius  $g$ , having the angular displacement  $(\mu\theta + \alpha)$ . Then, let us call the zone enclosed by  $\eta = y_0 \pm 1$  as "stop region," and those totally outside the zone thereof as "start region" as shown in Fig. 5. With these propositions, the condition of "start" or "stop" can be summarized as follows:

When the point  $s_0''$  comes into the stop region, the motion stops and when it falls in the start region, the motion starts. When the point  $s_0''$  just comes on the boundary, two cases are discriminated. If the point  $e$  rotating from  $s_0''$  as a starting point enters the stop region, the motion stops, and if it enters the start region, the motion starts. When the motion starts, the sign of corresponding velocity thereafter would be determined by that of  $w_0$ .

### 2.3. Topological Curve after Switching

The motion of vibrational system should be continuous in its velocity and displacement before and after switching regardless of start or stop. Let the concerned symbol for motion just before and after switching be represented by "0" and "1", respectively. Then,

$$\text{and} \quad \left. \begin{array}{l} y_0 = y_1, \\ \dot{y}_0 = \dot{y}_1. \end{array} \right\} \quad (50)$$

Since the last term of Eq. (5) representing harmonic external force is always continuous, we have

$$\text{and } \left. \begin{aligned} v_0 &= v_1, \\ \dot{v}_0 &= \dot{v}_1. \end{aligned} \right\} \quad (51)$$

Substituting (50) and (51) into (15) and (16), we obtain

$$\text{and } \left. \begin{aligned} u_0 &= y_0 - \frac{v_0}{\gamma} = u_1, \\ \dot{u}_0 &= \dot{y}_0 - \frac{\dot{v}_0}{\gamma} = \dot{u}_1. \end{aligned} \right\} \quad (52)$$

Equations (51) and (52) indicate that the values of  $u$ ,  $\dot{u}$  and  $v$  before and after switching are continuous, and the switching points on the topological curve after switching are the points just before switching.

When the point  $s_0''$  enters the start region and the value of  $w_0$  is determined, the center of spiral curve in  $u-\dot{u}$  plane can be located, and we can then draw a spiral curve so that it passes through the point  $s_0$ . The point  $q$  starts from  $s_0'$  in  $\dot{u}-v$  plane, thus, a topological curve in the plane can be drawn in the way as described in the preceding paragraph.

When the point  $s_0''$  comes into the stop region, a discrimination is to make to see whether it accompanies a permanent stop or a temporary one. The condition for the permanent one is that the circle in  $\xi-\eta$  plane is completely included in the suspending region.

When a part of the circle in  $\xi-\eta$  plane exists in the start region and  $s_0''$  falls in the stop region, the motion is brought to a temporary stop until the moving point  $e$  comes out of the stop region.

In order to indicate above-mentioned functions concretely, suppose that the switching points  $s_0$ ,  $s_0'$  and  $s_0''$  have been determined in each plane as illustrated in Fig. 6. In this case, however, the motion stops since the point  $s_0''$  locates in the stop region. But, at a moment when the moving point  $e$  which starts its rotation from the point  $s_0''$  in a clockwise direction reaches the point  $I_1$ , the external force that would be applied thereafter becomes positive (negative for  $J_2$ ), with the result that the system thereafter is set in motion with positive velocity. The point  $I_1$  is also the switching point  $s_2''$  for starting motion. Denote  $s_2'$  an intersecting point of the circle in  $\dot{u}-v$  plane with  $o's_2'$  drawn parallel to  $o's_2''$ , then, the point  $s_2'$  becomes the switching point for starting motion in this plane. Let  $\dot{u}_2$  and  $v_2$  be co-ordinates of the point  $s_2'$ , then, from

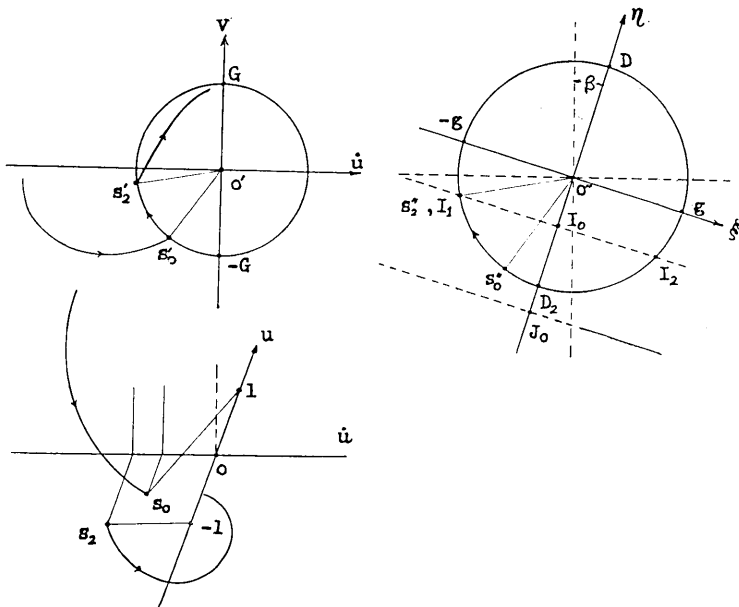


Fig. 6.

$$u_2 = y_0 - \frac{v_2}{\gamma} = u_0 + \frac{(v_0 - v_2)}{\gamma}, \tag{53}$$

and together with  $\dot{u}_2$ , the switching point  $s_2$  in  $u-\dot{u}$  plane is determined. Since the velocity expected thereafter is positive in this case, the topological curve in this plane is a logarithmic spiral having its center at the point  $u = -1$  and passing through  $s_2$ .

The discussion made thus far does not touch on the method of drawing a curve connecting both points  $s_0$  and  $s_2$ , no need, however, is called for in this regard since the point  $s_2$  is obtained without an actual drawing.

In addition to the above, a consideration will be paid to the topological curve in  $\dot{u}-v$  plane when the motion is stopping. Through the meaning of both Exps. (19) and (27), we can understand that a topological point moves on the circle with radius  $G$  in a clockwise direction.

### CHAPTER III. SOLUTION UNDER STEADY STATE

#### 3.1. Solution

A detailed discussion has thus far been developed on the method of

drawing topological curves to indicate the motion of the mass. Continuation of proposed procedure would finally fall in the case of permanent stop or would approach to a constant closed curve, which corresponds to the limit cycle for the desired solution under a steady state. From such a limit cycle, the maximum value of displacement and the phase difference between external force and its corresponding displacement can be made known.

Fig. 7 shows the limit cycle corresponding to the case  $g=2.0$ ,  $h=0.2$  and  $\mu=1.25$ , in which  $s_0$  and  $s'_0$  are the switching points, at which  $y$  becomes its maximum value  $y_{max}$ . By measuring the coordinates of  $s'_0$  and  $s''_0$  in Fig. 7

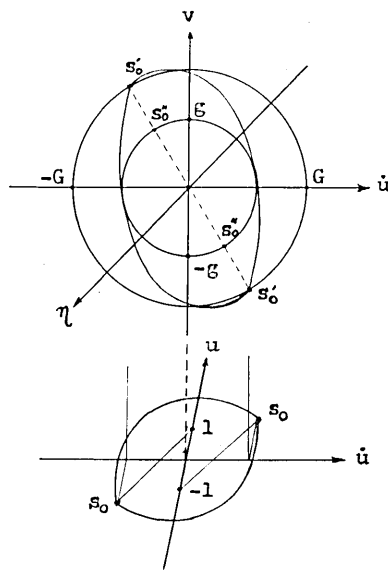


Fig. 7.

$y_{max}$  can be obtained from the following equation derived from (43),

$$y_{max} = u\text{-component of } s_0 + \frac{(v\text{-component of } s'_0)}{\gamma} \quad (54)$$

Let the switching point be taken as an origin of time, then, we can understand from (42),

$$\alpha = \angle \gamma o' s'_0 \quad (55)$$

This means that the phase difference  $\alpha$  can be measured as an angle between  $\gamma$ -axis and  $o' s'_0$ , the clockwise direction being positive.

The above example does not include any existence of temporary stop, however, there are some cases where the limit cycle can be obtained for such steady motion which includes repetition of temporary stop. This case as illustrated by Fig. 8, in

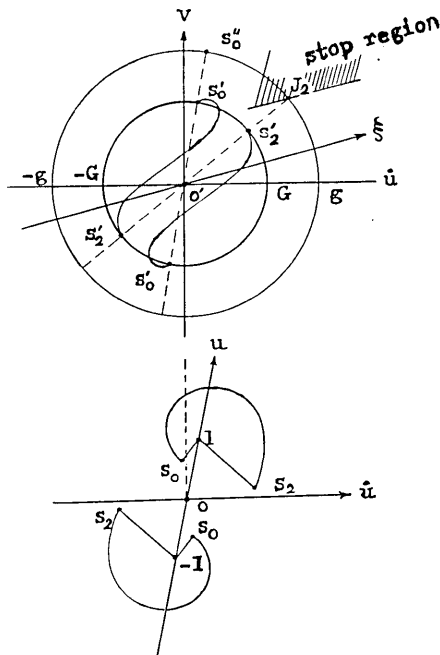


Fig. 8.



which Exp. (54) is of a direct use to obtain the maximum displacement  $y_{max}$ . For convenience, in this case, let us take the origin of time at the beginning of suspending interval on  $y_{max}$ . This means, in Fig. 8, the moment that the rotating point  $q$  coincides with  $s'_0$ . Then, the same expression as (55) is usable to know the phase angle  $\alpha$  graphically.

3.2. Discussion

Now, let us compare the results obtained graphically with those obtained theoretically by T. Hagiwara<sup>8)</sup>. His theoretical formulas with notations used in this paper are

$$\left. \begin{aligned}
 g &= y_{max} \sqrt{\{(1-\gamma^2)A'_1 + 2h\gamma B'_1\}^2 + \left\{-(1-\gamma^2)B'_1 + 2h\gamma A'_1 + \frac{4}{\pi y_{max}}\right\}^2} \\
 \tan \alpha &= \frac{-(1-\gamma^2)B'_1 + 2h\gamma A'_1 + \frac{4}{\pi y_{max}}}{(1-\gamma^2)A'_1 + 2h\gamma B'_1} \\
 A'_1 &= 1 + \frac{S_A}{y_{max}} \\
 B'_1 &= \frac{S_B}{y_{max}}
 \end{aligned} \right\} \quad (56)$$

Now, in order to compare both results, five cases will be considered. Put the value  $y_{max}=1.15$  obtained graphically into (56) and calculate  $g$  and  $\tan \alpha$  by using the values  $S_A=0.00436$  and  $S_B=0.197$ . Then, we can compare the values  $g$  and  $\alpha$  on both methods as shown in the case (1) of Table 2. In cases (2) and (3) such can be done. These three

Table 2.

Case	$g$	$h$	$\mu$	$S_A$	$S_B$	Eqs. (56)'s		Graphical	
						$g$	$\alpha$	$g$	$\alpha$
(1)	2.0	0.2	1.25	.00436	0.197	1.996	103.9°	2.0	104.5'
(2)	2.0	0.2	1.00	.00901	0.313	2.003	84.3°	2.0	84.2'
(3)	4.0	0.4	1.00	.02300	0.360	3.978	77.7°	4.0	77.7'
(4)	2.0	0.2	0.50	.14200	1.594	1.862	13.9°	2.0	23.5'
(4')	2.0	0.2	0.50	.14200	1.594	1.985	14.0°	2.0	14.5'
(5)	4.0	0.4	0.50			3.98	25.6°	4.0	26.0'
(5')	4.0	0.4	0.50			4.00	25.6°	4.0	24.9'

8) *loc. cit.*, 2).

cases show a satisfactory coincidence between the two methods: All of these, however, do not include any temporary stop. Therefore, a need is called for to make further analytical comparison on such a case as includes a temporary stop.

For  $g=2$ ,  $h=0.2$  and  $\mu=0.5$ , which correspond to the case of Fig. 8, the results in case (4) of Table 2 reveal a considerable amount of difference between the two solutions under a steady state when the motion includes temporary stop. In order to clarify the cause of such discrepancy on both results, an attempt is made here to obtain the solution of steady motion graphically as discussed in this paper under the assumption that  $r$  changes immediately as soon as the velocity becomes zero, and to compare the results with those obtained by (56).

If the change of  $r$  is assumed as above, the graphical tracing can be made much simplified, and discrimination of the conditions with regard to "start" or "stop" thereby being eliminated. Correspondingly, no consideration is required as to the circle of radius  $g$ , which leads to an absolute jump of the center of spiral from  $+1$  to  $-1$  or *vice versa* after the determination of switching point.

The limit cycle thus traced is shown in Fig. 9. The value  $y_{\max}$  is thereby measured in Fig. 9, which is in turn put into (56) to calculate  $g$  and  $\alpha$ . The results for comparison are shown in the case (4) of Table 2, from which we find that two results are in satisfactory coincidence. After all, the cause of discrepancy appearing in this case is undoubtedly due to the assumption of friction when the system is at rest. The limit cycle obtained graphically in case (5) of Table 2 also includes temporary stop. The comparison of the results show a discrepancy, too. But, the results shown in the case (5) which is obtained graphically without discrimination of conditions is also in good coincidence.

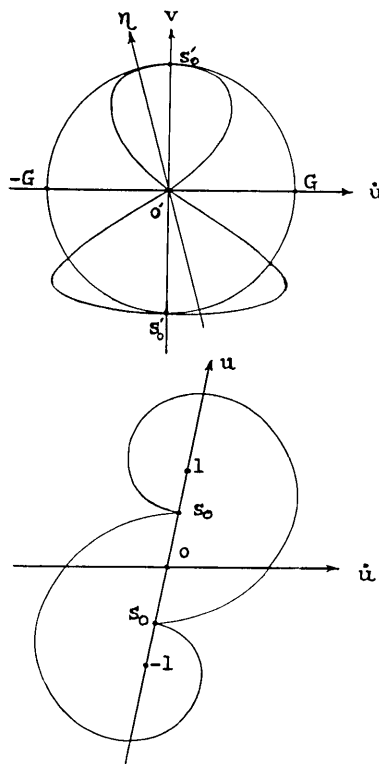


Fig. 9.

As a conclusion, it can be said that the graphical method stated in this Part is usable to solve the problem, not only when the steady motion becomes continuous vibration, but also when it involves temporary stop. As a matter of fact, it is a complicated matter to solve the problem by analytical method using a directly derived solution from the equation of motion, especially, in the case of vibration with temporary stop. However, we can avoid this difficulty by using an electronic computer, and such a method will be stated in the following Part.

## Part II. Theory of Analytical Method

### 1. Introduction

When a system with one degree of freedom is set in motion by an external harmonic force under the existence of both solid and fluid frictions, the vibration remains continuous when the amplitude of external force is sufficiently great compared with the magnitude of the solid friction. J. P. Den Hartog<sup>9)</sup> has treated this case analytically and has influenced the following formulas starting from a directly derived solution of the equation of motion:

$$\left. \begin{aligned} y_{\max} &= -B_1 + \sqrt{(eg)^2 + B_2^2}, \\ \sin(\alpha + \beta) &= \frac{-B_2}{eg}, \text{ and } \cos(\alpha + \beta) = \frac{(y_{\max} + B_1)}{eg}, \end{aligned} \right\} \quad (57)$$

where

$$\left. \begin{aligned} B_1 &= \frac{\nu \sinh\left(\frac{h\pi}{\gamma}\right) - h \sin\left(\frac{\nu\pi}{\gamma}\right)}{\nu \left\{ \cosh\left(\frac{h\pi}{\gamma}\right) + \cos\left(\frac{\nu\pi}{\gamma}\right) \right\}}, \\ B_2 &= \frac{\sin\left(\frac{\nu\pi}{\gamma}\right)}{\nu \gamma \left\{ \cosh\left(\frac{h\pi}{\gamma}\right) + \cos\left(\frac{\nu\pi}{\gamma}\right) \right\}}, \end{aligned} \right\} \quad (58)$$

The notations which were used in the above formulas and which will be used from now on are the same as those in the preceding Part, unless otherwise specified.

9) *loc. cit.*, 1).

## 2. Conditions of Steady State for Vibration with Temporary Stop

When the external force is made smaller and comes in the neighborhood of the magnitude of the solid friction, a certain stopping interval would become apparent during a period of vibration and such steady motion would continue. In such a case, a prediction will be made possible as to the change of  $y$  and  $R$ , and it is summarized as follows:

i) Periods of vibrations of  $y$  and  $R$  would be the same as that of external force.

ii) Since it is natural to assume that  $y$  and  $R$  in two intervals, in which positive and negative directions of external force are acting, have the same magnitude of variation with opposite sign,

$$\left. \begin{aligned} y(\gamma\tau + \pi) &= -y(\gamma\tau), \\ \text{and } R(\gamma\tau + \pi) &= -R(\gamma\tau). \end{aligned} \right\} \quad (59)$$

iii) During the moving interval,  $y$  is governed by Eq. (5) and  $R = \pm 1$ .

iv) During the stopping interval,  $y = \pm y_{\max}$ , and  $R$  changes as shown in (8).

Let us take  $\gamma\tau = 0$  as the moment when the motion has just stopped, further, the stopping and moving intervals be assumed as that,

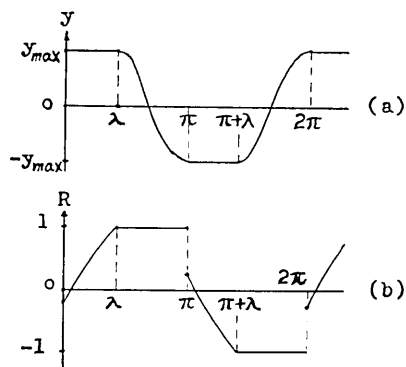


Fig. 10.

$$0 < \gamma\tau < \lambda, \quad (60)$$

$$\text{and } \lambda < \gamma\tau < \pi \quad (61)$$

respectively. Then, in consideration of those mentioned above, the variations of  $y$  and  $R$  can be graphically represented as shown in Figs. 10 (a) and (b). And, it indicates that a basic interval is

$$0 < \gamma\tau < \pi. \quad (62)$$

By shifting one cycle of the interval as well as reversing the sign, the following variation corresponding to the interval,

$$\pi < \gamma\tau < 2\pi$$

can be obtained. This means that the basic interval (62) alone is sufficient enough for the development of a discussion regarding the steady state.

3. Solution of problem

The basic interval referred to in the preceding paragraph can be divided into two groups, *i.e.*, stopping and moving intervals.

In the stopping interval, the variation of  $y$  and  $R$  are

$$\left. \begin{aligned} y &= y_{\max}, \\ R &= y_{\max} - g \cos(\gamma\tau + \alpha). \end{aligned} \right\} \quad (63)$$

Furthermore, the boundary condition regarding the solid friction will be,

$$\text{when } \gamma\tau = 0, \quad R = R_0,$$

$$\text{and when } \gamma\tau = \lambda, \quad R = 1.$$

Substituting above conditions to (63), we have

$$R_0 = y_{\max} - g \cos \alpha, \quad (64)$$

$$y_{\max} = 1 + g \cos(\lambda + \alpha). \quad (65)$$

In the moving interval, since  $R$  is assumed as  $+1$ , the solution of the equation of motion (5) can be written with two integral constants  $C_1$  and  $C_2$  in the following form:

$$y = \exp(-h\tau)(C_1 \cos \nu\tau + C_2 \sin \nu\tau) + (A \cos \gamma\tau + B \sin \gamma\tau) \cos \alpha + (B \cos \gamma\tau - A \sin \gamma\tau) \sin \alpha + 1. \quad (66)$$

And, its differentiation with regard to  $\tau$  is

$$\dot{y} = \exp(-h\tau)\{C_2(\nu \cos \nu\tau - h \sin \nu\tau) - C_1(h \cos \nu\tau + \nu \sin \nu\tau)\} + \gamma \cos \alpha(B \cos \gamma\tau - A \sin \gamma\tau) - \gamma \sin \alpha(A \cos \gamma\tau + B \sin \gamma\tau), \quad (67)$$

in which  $A$  and  $B$  are

$$A = \frac{(1 - \gamma^2)g}{(1 - \gamma^2)^2 + (2h\gamma)^2}, \quad B = \frac{2h\gamma g}{(1 - \gamma^2)^2 + (2h\gamma)^2}. \quad (68)$$

Before and after the concerned interval, conditions with regard to the displacement and the velocity of the system are given as

$$\text{when } \gamma\tau = \lambda, \quad y = y_{\max}, \quad \text{and } \dot{y} = 0,$$

$$\text{and when } \gamma\tau = \pi, \quad y = -y_{\max}, \quad \text{and } \dot{y} = 0.$$

Applying above four conditions to (66) and (67), we have

$$\left. \begin{aligned} C_1 T_1 + C_2 T_2 &= y_{\max} - T_3 \cos \alpha - T_4 \sin \alpha - 1, \\ C_1 T'_1 + C_2 T'_2 &= -y_{\max} - T'_3 \cos \alpha - T'_4 \sin \alpha - 1, \end{aligned} \right\} \quad (69)$$

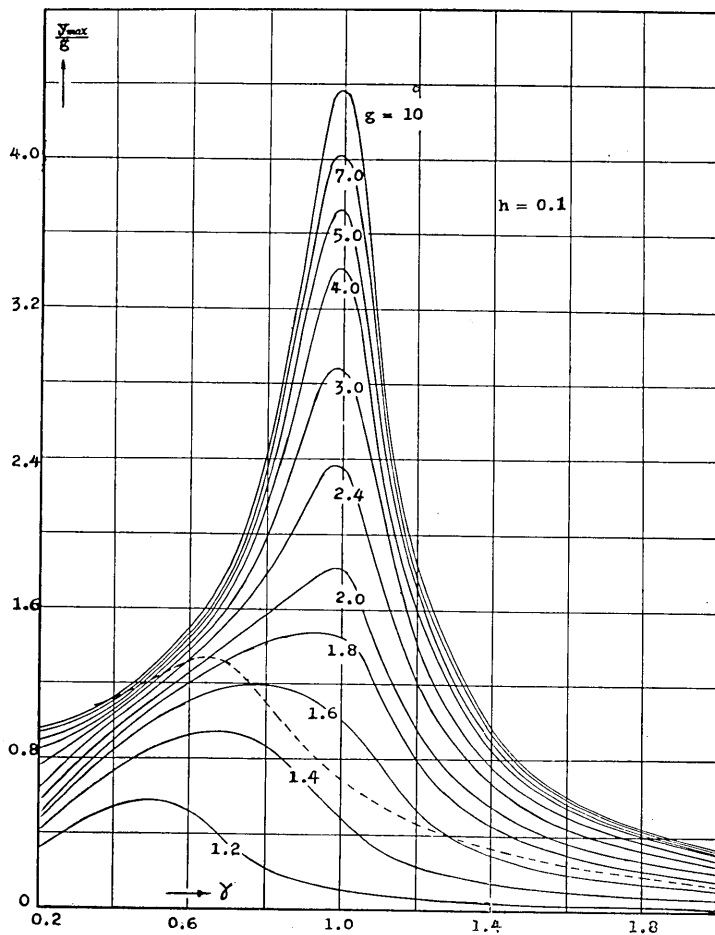


Fig. 11.

$$\left. \begin{aligned} C_1 T_5 + C_2 T_6 &= \gamma (T_4 \cos \alpha - T_3 \sin \alpha), \\ C_1 T'_5 + C_2 T'_6 &= \gamma (T'_4 \cos \alpha - T'_3 \sin \alpha), \end{aligned} \right\} \quad (70)$$

where

$$\left. \begin{aligned} T_1 &= \exp\left(\frac{-h\lambda}{\gamma}\right) \cos\left(\frac{\nu\lambda}{\gamma}\right), & T'_1 &= \exp\left(\frac{-h\pi}{\gamma}\right) \cos\left(\frac{\nu\pi}{\gamma}\right), \\ T_2 &= \exp\left(\frac{-h\lambda}{\gamma}\right) \sin\left(\frac{\nu\lambda}{\gamma}\right), & T'_2 &= \exp\left(\frac{-h\pi}{\gamma}\right) \sin\left(\frac{\nu\pi}{\gamma}\right), \\ T_3 &= A \cos \lambda + B \sin \lambda, \end{aligned} \right\} \quad (71)$$

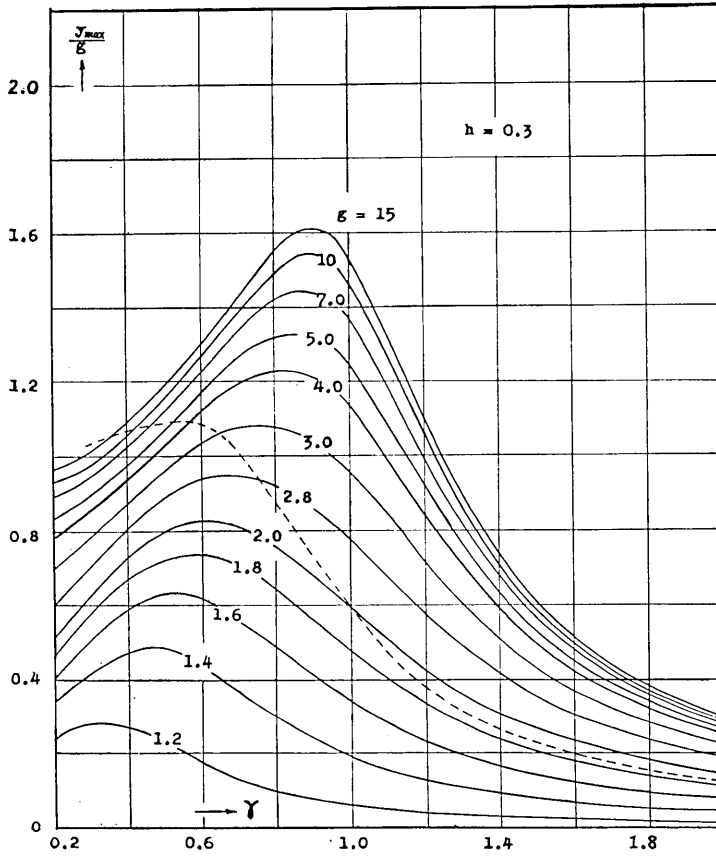


Fig. 12.

$$T_4 = B \cos \lambda - A \sin \lambda,$$

$$T_5 = hT_1 + \nu T_2,$$

$$T_6 = hT_2 - \nu T_1,$$

$$T'_5 = hT'_1 + \nu T'_2,$$

$$T'_6 = hT'_2 - \nu T'_1.$$

We can obtain  $C_1$  and  $C_2$  from Eqs. (69) as under:

$$\left. \begin{aligned} C_1 &= \frac{U_1 y_{max} + U_2 + U_3 \cos \alpha + U_4 \sin \alpha}{U_5}, \\ C_2 &= -\frac{U'_1 y_{max} + U'_2 + U'_3 \cos \alpha + U'_4 \sin \alpha}{U_5}, \end{aligned} \right\} \quad (72)$$

where

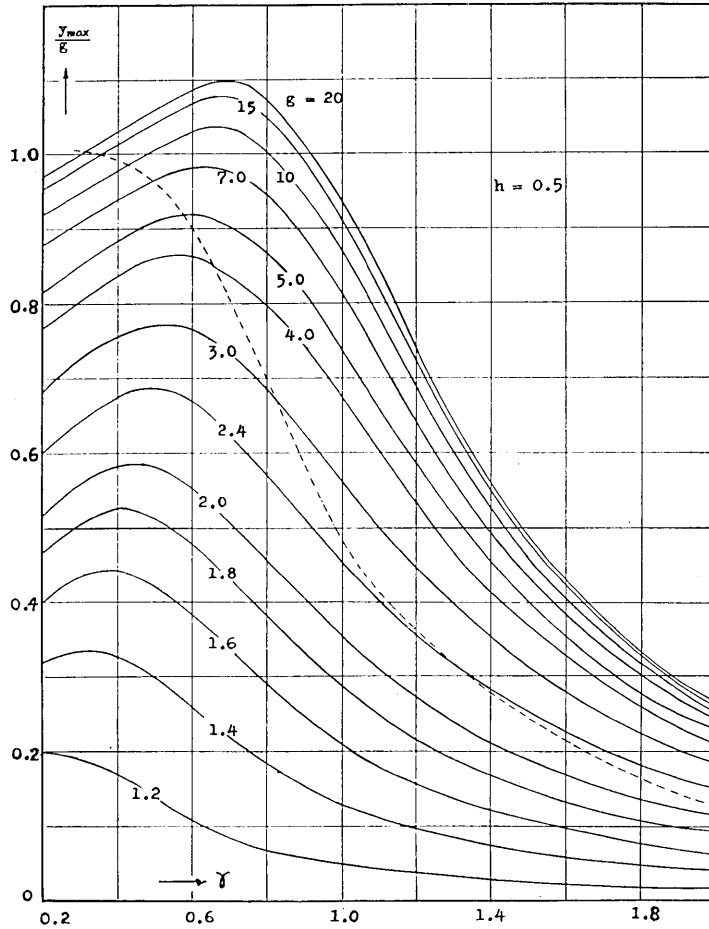


Fig. 13.

$$\left. \begin{aligned}
 U_1 &= T_2 + T'_2, & U'_1 &= T_1 + T'_1, \\
 U_2 &= T_2 - T'_2, & U'_2 &= T_1 - T'_1, \\
 U_3 &= -AT_2 - T'_2T_3, & U'_3 &= -AT_1 - T'_1T_3, \\
 U_4 &= -BT_2 - T'_2T_4, & U'_4 &= -BT_1 - T'_1T_4, \\
 U_5 &= T_1T'_2 - T'_1T_2.
 \end{aligned} \right\} \quad (73)$$

Substituting (72) into (70), we have

$$\left. \begin{aligned}
 y_{max} &= \frac{V_1 \cos \alpha + V_2 \sin \alpha + V_3}{V_4}, \\
 y_{max} &= \frac{V'_1 \cos \alpha + V'_2 \sin \alpha + V'_3}{V'_4},
 \end{aligned} \right\} \quad (74)$$



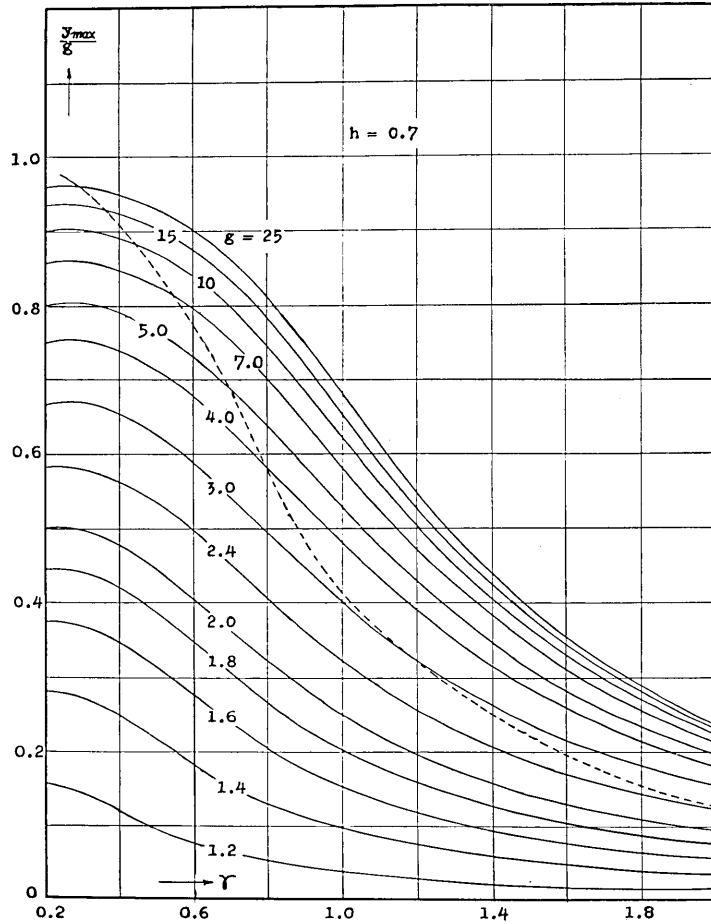


Fig. 14.

where

$$\left. \begin{aligned} V_1 &= U_3 T_5 - U_3 T_6 - \gamma U_5 T_4, & V'_1 &= U_3 T'_5 - U_3 T'_6 + \gamma B U_5, \\ V_2 &= U_4 T_5 - U_4 T_6 + \gamma U_5 T_3, & V'_2 &= U_4 T'_5 - U_4 T'_6 - \gamma A U_5, \\ V_3 &= U_2 T_5 - U_2 T_6, & V'_3 &= U_2 T'_5 - U_2 T'_6, \\ V_4 &= U_1 T_6 - U_1 T_5, & V'_4 &= U_1 T'_6 - U_1 T'_5. \end{aligned} \right\} \quad (75)$$

Eliminating  $y_{max}$  from Eqs. (65) and (74), we have

$$\left. \begin{aligned} S_1 \cos \alpha + S_2 \sin \alpha &= S_3, \\ S'_1 \cos \alpha + S'_2 \sin \alpha &= S'_3, \end{aligned} \right\} \quad (76)$$

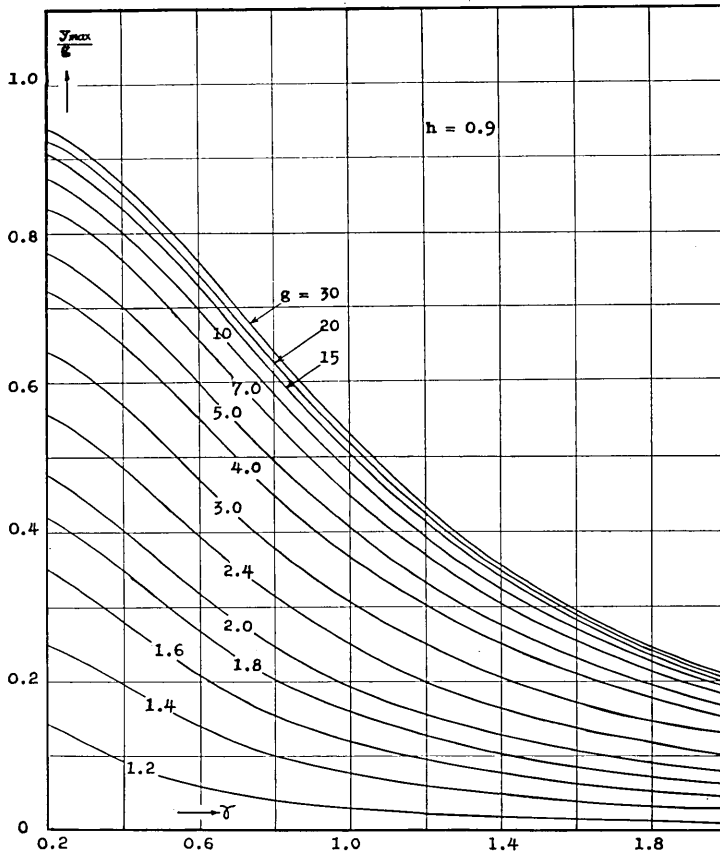


Fig. 15.

where

$$\left. \begin{aligned} S_1 &= V_1 - gV_4 \cos \lambda, & S'_1 &= V'_1 - gV'_4 \cos \lambda, \\ S_2 &= V_2 + gV_4 \sin \lambda, & S'_2 &= V'_2 + gV'_4 \sin \lambda, \\ S_3 &= V_4 - V_3, & S'_3 &= V'_4 - V'_3. \end{aligned} \right\} \quad (77)$$

From (76), we can obtain

$$\left. \begin{aligned} \sin \alpha &= \frac{S_1 S'_3 - S'_1 S_3}{S_1 S'_2 - S'_1 S_2}, \\ \cos \alpha &= -\frac{S_2 S'_3 - S'_2 S_3}{S_1 S'_2 - S'_1 S_2}. \end{aligned} \right\} \quad (78)$$

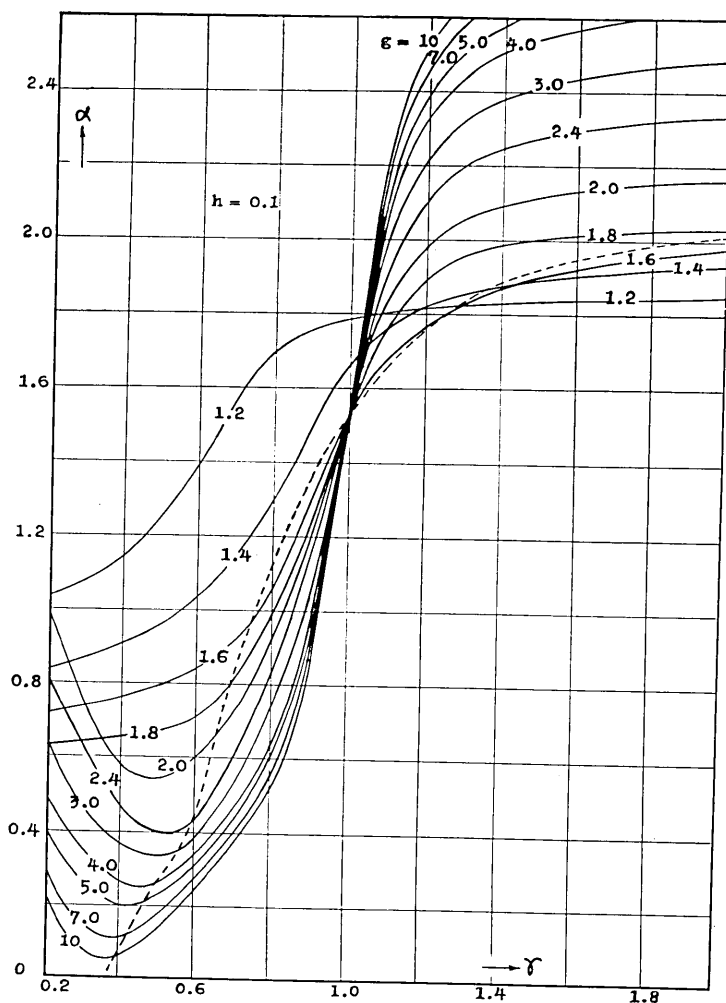


Fig. 16.

Eliminating  $\sin \alpha$  and  $\cos \alpha$  from above equations, we have

$$(S_1 S'_2 - S'_1 S_2)^2 = (S_1 S'_3 - S'_1 S_3)^2 + (S_2 S'_3 - S'_2 S_3)^2. \quad (79)$$

Since Eq. (79) has only the variable  $\lambda$ , we can obtain its value as the root of Eq. (79). With  $\lambda$  thus obtained, firstly  $\alpha$  from (78), secondly  $y_{\max}$  from (65), thirdly  $R_0$  from (64) can be calculated.

Thus far, we have developed in the preceding paragraph a discussion on the general method of deriving a solution for steady motion. The

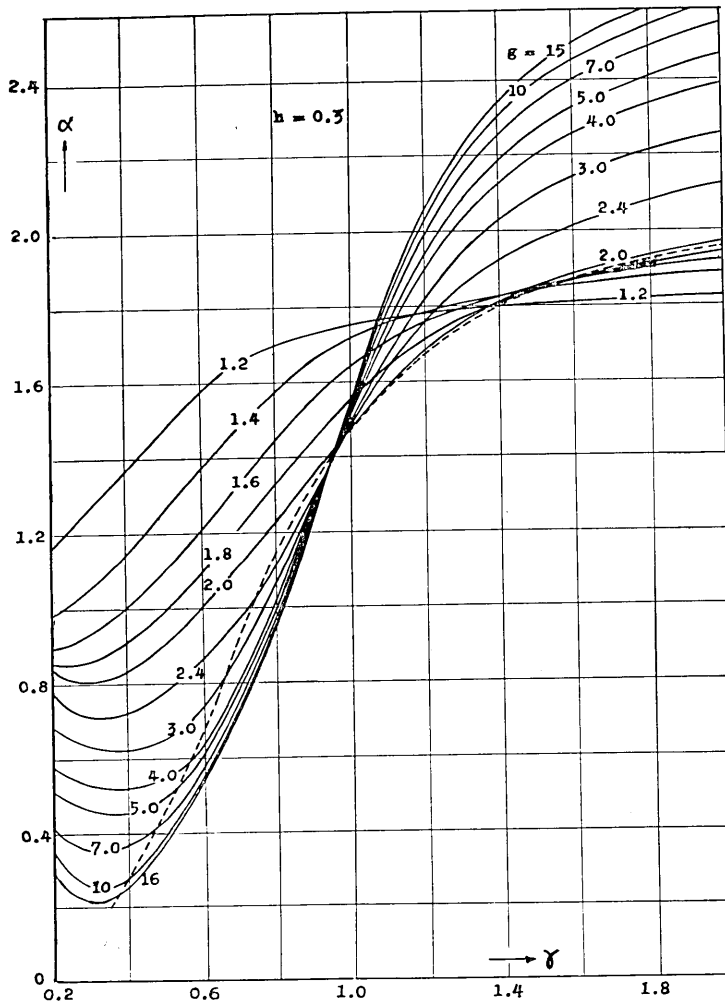


Fig. 17.

solution thus obtained by giving all possible arbitrary values of  $g$ ,  $h$  and  $\gamma$ , however, may not lead to the true solution of this problem. In this Part, a discussion is made assuming that the value of  $\lambda$  would fall in a zone, *i.e.*,

$$0 \leq \lambda \leq \pi, \quad (80)$$

no consideration being paid to the other value of  $\lambda$  than mentioned above. Therefore, the value of  $\lambda$  thus calculated is in need of selection to satisfy the condition (80).

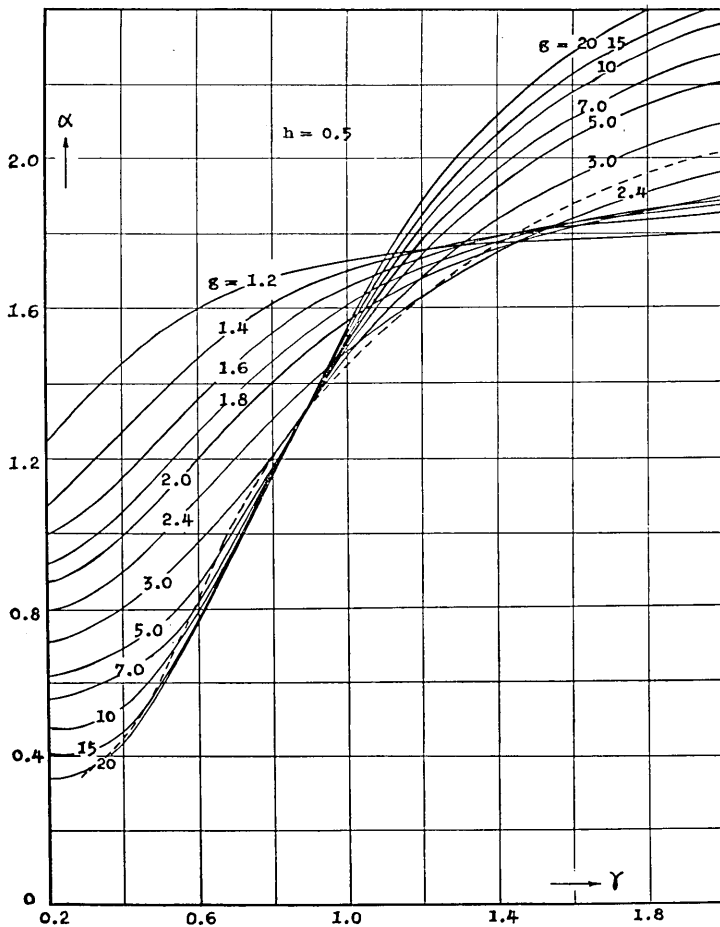


Fig. 18.

Among the values of  $g$ ,  $h$  and  $\gamma$ , for which an existence of actual solution for steady motion including temporary stop can be promised, let  $h$  and  $\gamma$  be constant and  $g$  made gradually greater, the stopping interval  $\lambda$  is then supposed to become gradually smaller to reach zero finally. Since the limit  $\lambda=0$  is considered to be exactly on the boundary of two, *i.e.*, one including stopping interval and the other zero or not, the condition to be satisfied at such a boundary should be found. For this purpose, putting  $\lambda=0$  into (71), and carrying out the same calculation as described from (72) to (79), instead of Eq. (79), we can obtain

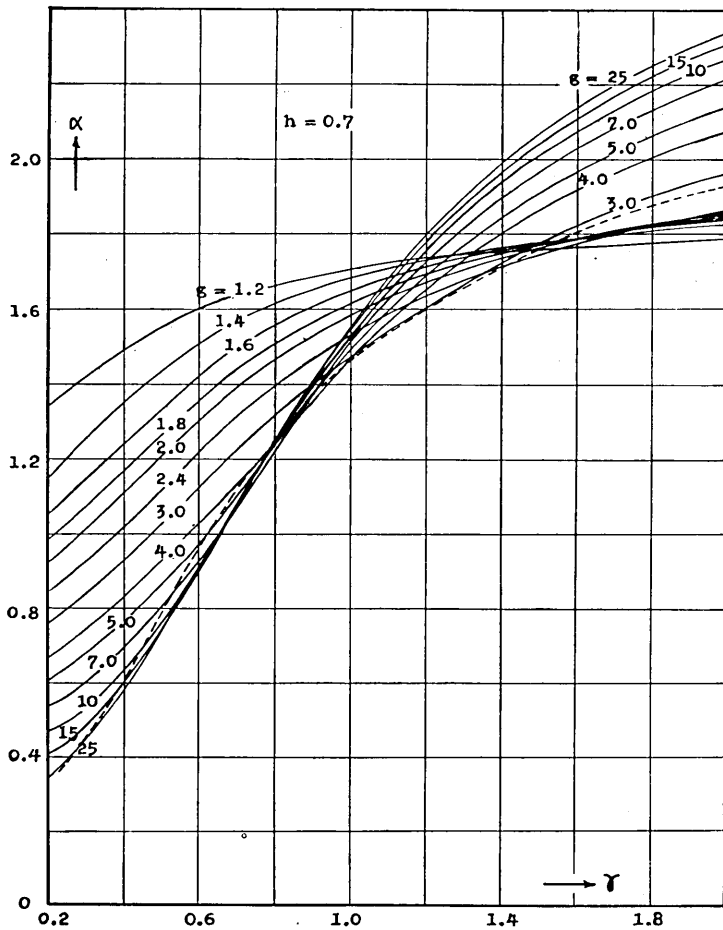


Fig. 19.

$$\frac{1}{4}\{B^2 - (g-A)A\}^2\{T'_2(h-T'_0) - (1+T'_1)(\nu-T'_0)\}^2\gamma^2$$

$$= (g-A)(hT'_0 - \nu T'_0) + \gamma(\nu - T'_0)^2 + \{\gamma A(\nu - T'_0) + B(hT'_0 + \nu T'_0)\}^2. \quad (81)$$

This is the equation giving the relation between  $g$ ,  $h$  and  $\gamma$  at the boundary.

#### 4. Frequency Response

Results obtained by the above stated method are given in Figs. 11-20. Among them, response curves shown in Figs. 11-15 are the relationships between the relative frequency  $\gamma$  and the relative maximum amplitude

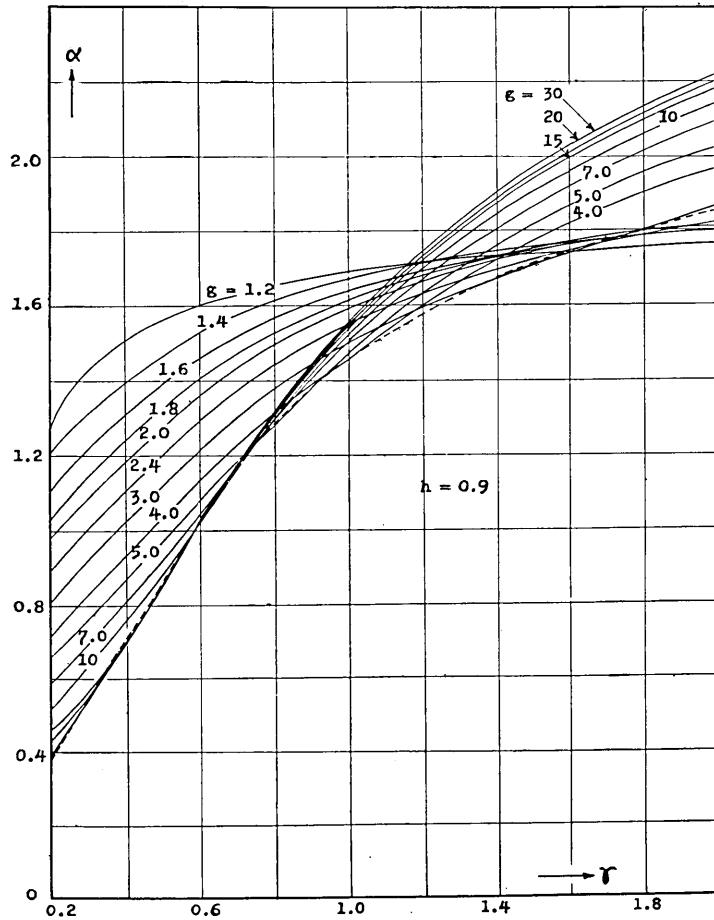


Fig. 20.

$\frac{y_{max}}{g}$  with  $g$  as a parameter. The relationships of the relative frequency and the angle of phase difference  $\alpha$  are shown in Figs. 16-20. In Figs. 11-20, the dotted line indicates the border-line between the continuous vibrations and the steady vibrations with one stop in a half period, being obtained as follows: Using the constant values of  $g$  and  $h$ , the value of  $\gamma$  is obtained from Eq. (81), and these three values are applied to the formulas (57) of J. P. Den Hartog, therefore, we can calculate  $\frac{y_{max}}{g}$  and  $\alpha$  as the boundary values.

With regard to the curves for the relative amplitude, upper lines above the boundary-line correspond to the continuous vibration, and are

the results from (57). Lines lower than the boundary correspond to a temporary stopping vibration, and are the results from the method developed in the preceding paragraph.

In this Part, the discussion has been developed under the assumption of stationary vibration with only one time interval of stop during a half period. Accordingly, all results obtained here were solutions corresponding to one stop. Thomas A. Parls and Emile S. Herrard<sup>10)</sup> have, however, pointed out that stationary vibrations having two or more stops in a half period are possibly in existence.

### Part III. Theory of Analytical Method

The theory developed in the preceding Part with regard to the analytical method obtaining the solution under steady state corresponds to the case where  $h$  is smaller than unity. In the other case, an application of a different type of solution would be required. Here will be explained another analytical method of solving the problem with Fourier series which allows no consideration of the value of  $h$ .

As described in Eq. (59) of Part I, the following conditions exist under the steady motion:

$$\left. \begin{aligned} y(\phi + \pi) &= -y(\phi), \\ R(\phi + \pi) &= -R(\phi), \end{aligned} \right\} \quad (82)$$

where  $\phi = \gamma\tau$ . (83)

The variations of  $y$  and  $R$  under steady state can be expressed in the terms of Fourier series, in which the terms of even number would disappear through the characteristic indicated by (82), *i.e.*,

$$y = \sum_{N=0}^{\infty} \{A_{2N+1} \cos (2N+1)\phi + B_{2N+1} \sin (2N+1)\phi\}, \quad (84)$$

$$R = \sum_{N=0}^{\infty} \{C_{2N+1} \cos (2N+1)\phi + D_{2N+1} \sin (2N+1)\phi\}, \quad (85)$$

where the coefficients  $C_{2N+1}$  and  $D_{2N+1}$  provide the following relation:

$$\left. \begin{aligned} C_{2N+1} &= \frac{2}{\pi} \int_0^{\pi} R \cos (2N+1)\phi \alpha \phi, \\ D_{2N+1} &= \frac{2}{\pi} \int_0^{\pi} R \sin (2N+1)\phi \alpha \phi. \end{aligned} \right\} \quad (86)$$

10) *loc. cit.*, 3).



The value of  $R$  under steady state can be assumed as described in Part I;

$$\left. \begin{aligned} &\text{when } 0 < \phi < \lambda, \quad R = y_{\max} - g \cos(\phi + \alpha), \\ &\text{and when } \lambda < \phi < \pi, \quad R = 1. \end{aligned} \right\} \quad (87)$$

Putting these relationships into (86), the results of calculation are as follows :

$$C_{2N+1} = \frac{2g \cos(\lambda + \alpha) \sin(2N+1)\lambda}{(2N+1)\pi} - \frac{g}{2\pi} \left[ \frac{\sin(2N\lambda - \alpha) + \sin \alpha}{N} + \frac{\sin\{2(N+1)\lambda + \alpha\} - \sin \alpha}{N+1} \right], \quad (88)$$

$$D_{2N+1} = \frac{2\{2 + g \cos(\lambda + \alpha) - g \cos(\lambda + \alpha) \cos(2N+1)\lambda\}}{(2N+1)\pi} + \frac{g}{2\pi} \left[ \frac{\cos(2N\lambda - \alpha) - \cos \alpha}{N} + \frac{\cos\{2(N+1)\lambda + \alpha\} - \cos \alpha}{N+1} \right], \quad (89)$$

In deriving above relationships,  $y_{\max}$  has been eliminated by applying (65).

Let us rewrite the expression (84) here again and differentiate with regard to  $\tau$ , thus, we have

$$\left. \begin{aligned} y &= \sum_{N=0}^{\infty} \{A_{2N+1} \cos(2N+1)\phi + B_{2N+1} \sin(2N+1)\phi\}, \\ \dot{y} &= \gamma \sum_{N=0}^{\infty} (2N+1) \{B_{2N+1} \cos(2N+1)\phi - A_{2N+1} \sin(2N+1)\phi\}, \\ \ddot{y} &= -\gamma^2 \sum_{N=0}^{\infty} (2N+1)^2 \{A_{2N+1} \cos(2N+1)\phi + B_{2N+1} \sin(2N+1)\phi\}. \end{aligned} \right\} \quad (90)$$

Putting above expressions into the equation of motion (5), and comparing the coefficients of sine and cosine terms, the results are obtained as,

i) for  $N > 0$ ,

$$\left. \begin{aligned} A_{2N+1} &= \frac{\{1 - (2N+1)^2 \gamma^2\} C_{2N+1} - 2h\gamma(2N+1)D_{2N+1}}{\{1 - (2N+1)^2 \gamma^2\}^2 + \{2h\gamma(2N+1)\}^2}, \\ B_{2N+1} &= \frac{2h\gamma(2N+1)C_{2N+1} + \{1 - (2N+1)^2 \gamma^2\} D_{2N+1}}{\{1 - (2N+1)^2 \gamma^2\}^2 + \{2h\gamma(2N+1)\}^2}, \end{aligned} \right\} \quad (91)$$

ii) for  $N = 0$ ,

$$\left. \begin{aligned} A_1 &= \frac{(1-\gamma^2)(C_1 + g \cos \alpha) - 2h\gamma(D_1 - g \sin \alpha)}{(1-\gamma^2)^2 + (2h\gamma)^2}, \\ B_1 &= \frac{2h\gamma(C_1 + g \cos \alpha) + (1-\gamma^2)(D_1 - g \sin \alpha)}{(1-\gamma^2)^2 + (2h\gamma)^2}. \end{aligned} \right\} \quad (92)$$

Therefore, the values of  $A_{2N+1}$  and  $B_{2N+1}$  have been expressed as functions of  $\alpha$  and  $\lambda$  under the given values of  $g$ ,  $h$  and  $\gamma$ .

When  $\phi = \lambda$ , or  $\phi = \pi$ ,  $\dot{y}$  should become zero. Applying these conditions to  $\dot{y}$  of Exp. (90), we have

$$\left. \begin{aligned} \sum_{N=0}^{\infty} (2N+1) \{ B_{2N+1} \cos (2N+1)\lambda - A_{2N+1} \sin (2N+1)\lambda \} &= 0, \\ \sum_{N=0}^{\infty} (2N+1) B_{2N+1} &= 0. \end{aligned} \right\} \quad (93)$$

The above two equations make up simultaneous equations with regard to  $\alpha$  and  $\lambda$ .

After obtaining the values of  $\alpha$  and  $\lambda$ ,  $y_{\max}$  can be calculated from Eq. (65), and further, the value of  $R_0$  can also be calculated from (64).

In this Part, we have developed a method to solve the problem by applying Fourier series and have derived the formulas to lead to a solution, but have not attained to numerical results. We assume that this kind of calculation is not so difficult when using an electronical computer.

#### 45. 調和型外力の作用する1自由度振動系における 固体摩擦の挙動

地震研究所 西村源六郎  
中央大学 小滝富雄

流体、固体両摩擦をうける1自由度の振動系に正弦的な外力が働くときの振動の問題を取扱い、固体摩擦としては運動時には一定値と仮定し、運動の向きによつてその符号が変わると考えた。なおこの他に静止時における摩擦力の性質をも考慮に入れた。

本文では問題を三つの方法で解き、各々の場合は第1部、第2部、第3部に分けられている。第1部では方程式から得られた解を逐次追跡していつて窮極的に定常解を得るという方法をとつた。この場合、計算の便宜のため、図式方法を導入した。その結果、強制力が小さくなると振動1周期の間に定常的に停止区間が現われることが示された。

第2部では停止区間をもつ定常解を仮定し、定常運動の条件から未定常数を求める方法をとつた。その結果得られる振幅、位相差、停止区間などの振動数レスポンスをグラフで与えた。

第3部では、やはり停止区間を想定した定常解をフーリエ級数で仮定し、定常運動の条件をつかつて運動を求める方法を示した。ここでは数値的な結果は省略した。